Larhyss Journal, ISSN 1112-3680, n°52, Dec 2022, pp. 29-47

EXPERIMENTAL STUDY OF THE HYDRAULIC JUMP COMPACTNESS IN THE COMPOUND RECTANGULAR CHANNEL

***BENMALEK A.* [1,2]*, *DEBABECHE M.* [2], *MEDJDOUB K.* [2], *MADI M.* [1], *HAFNAOUI M.A.* [1,2]**

[1] Scientific and Technical Research Center on Arid Regions C.R.S.T.R.A., Campus Mohamed Khider University, Biskra, Algeria
[2] Civil and Hydraulic Engineering, Laboratory of Research LARGHYDE, Mohamed Khider University, Biskra, Algeria

(*) *ahmed.benmalek@yahoo.fr*

Research Article – Available at http://larhyss.net/ojs/index.php/larhyss/index
Received June 11, 2022, Received in revised form December 3, 2022, Accepted December 5, 2022

ABSTRACT

The study of hydraulic jumps in compound rectangular channels has been the subject of several featured contributions. For hydrotechnical structures such as dams, this type of channel has been used in the design of energy dissipation basins to control the downstream flow discharge. In irrigation canals, this technique has presented a technical and economic advantage, especially in low-water periods where flow discharge has been widely exploited.

The main objective of this research is to find ways to exploit this configuration of the jump in future hydraulic designs. The present study is based on the experimental analysis of the hydraulic jump characteristics controlled by a thin sill evolving in a compound rectangular channel. This type of jump has been widely studied, and the current work focuses on the classical hydraulic jump.

Therefore, through this experimental contribution, the sill effect on the jump characteristics was analyzed. Moving the sill upstream caused jump compactness, defined by the length of the classical roller ratio and the geometric position of the sill. This phase of the flow leads to several jump configurations.

To achieve this objective, two cases were presented. In the first case, the flow takes place at the level of the minor bed of the channel with low Froude numbers. In the second case, the jump was formed at the level of the major bed where the Froude numbers are high. The jump compactness ratio was calculated in dimensionless terms as a function of the Froude number and the jump surface profile.

Keywords: Hydraulic jump, jump compactness, Froude number, compound rectangular channel, stilling basin.

INTRODUCTION

In nature, rivers are managed by two types of flows. The first occurs during the low-water period when flows are low, and the second occurs in the case of floods. The term "compound channel" covers channels of all cross sections having berms or floodplains (major bed), which come into action in the case of high flows but are normally dry. However, in the case of low flows, the flow occupies the bottom of the channel (minor bed).

The estimation of the various hydraulic parameters in compound channels has been the subject of extensive and fruitful contributions. This has led to the development of other physical aspects relating the channel shape to the different characteristics of flow.

Zahiri and Dehghani (2009) developed a model based on ANN (artificial neural networks) to estimate the flow rate of the right compound channels. After designing an optimal topology for the ANN model and the training process, the rest of the data sets were tested. The flow distribution along a compound prismatic channel was presented in the study by Bousmar et al. (2005). The authors estimated the required length of the channel, taking into account the actual development of the uniform flow at the surface of the water.

Liu et al. (2012) found that complex compound sections normally consist of several parts, so it is difficult to calculate the geometric parameters used to develop explicit equations for the critical depth. Therefore, the authors presented general equations for the geometric elements of these cross-sections. Based on the principle of progressive optimization adjustment and the theory of iteration, explicit equations have been developed for the direct calculation of the critical depth.

The phenomenon of the classical hydraulic jump in rectangular channels has been widely studied. The results obtained were beneficial for the design of energy dissipation basins. Bidone (1819) was the first to give the measurement and description of the hydraulic jump phenomenon. Later, Bélanger (1828), for the first time, presented a mathematical expression as the sequence depth ratio of the jump by using the momentum equation in a rectangular horizontal channel. Meanwhile, Bakhmeteff and Matzake (1936) conducted experiments on sloping channels and proposed dimensions of the water surface profile; they presented experimental data for the sequent depth ratio and the length of the jump in a rectangular channel.

Similarly, Moore (1943) studied the formation of the jump based on waterfalls. A simple experimental formula was developed by Hager (1993) for the surface profile of a hydraulic jump evolving in a rectangular channel. This new approach takes into account the roll length. The surface profile obtained corresponds well to existing data for Froude numbers varying from 2 to 10. Using the momentum equation of Yasuda and Hager

(1996), a relation for the sequence depth ratio is determined and verified with extended experiments. The wall surface profile is shown to be similar to and equal to the profile of the classical hydraulic jump. Roller and jump lengths were determined, and substantial agreement with the classical jump was again found.

Experiments were carried out in a horizontal rectangular channel by Wang and Chanson (2015). The authors examined in detail the fluctuations of the roller surface as well as the two-phase flow properties. The study was based on experimental results carried out in a relatively large installation covering a wide range of Froude numbers ($3.80<Fr_1<8.50$). A recent experimental contribution presented by Achour et al. (2022a) concerned the controlled hydraulic jump by a thin sill in a rectangular channel. The study was based on the determination of the value of the sill position X for the hydraulic jump to be completely formed in the stilling basin, where Lj is approximately equal to X. The hydraulic jump in the rectangular channel has been widely studied by Achour et al. (2022b, 2022c). The authors also analyzed the jump compactness effect by considering the length of the classic jump, *Lj**.

The hydraulic jump in trapezoidal channels is of additional interest with regard to the dissipation of energy in relation to the jump in rectangular channels (Kateb et al., 2013). The observations of Wanoschek and Hager (1989) have shown that the behavior of the jump in trapezoidal channels is different from that encountered in rectangular and triangular channels. This is mainly attributed to the existence of a bottom roller. The authors analyzed the main flow properties, such as the sequence height, length of the bottom roller and length characteristics.

Concerning the behavior of the jump in the enlarged trapezoidal channel, Omid et al. (2007) showed that the dissipation basins of trapezoidal shape gradually expanding with a given side slope lead to reduced sequence depth and jump length and increased energy loss compared to those observed in classical rectangular or trapezoidal cross-section channels. However, in compound rectangular channels, this phenomenon has inherent complexity. The difficulty of the problem is due to the implicit interaction between the flood plains and the main channel, characterizing each particular form of composite channel. An abruptly enlarged trapezoidal channel was investigated by Benmalek and Debabeche (2022), who evaluated the effect of the enlargement on the sequence depth ratio, the relative energy loss, and the jump surface profile.

Among the most recent works in this area are those of Khattaoui and Achour (2012) on the hydraulic jump in a compound rectangular channel. In this study, the authors found that uniform flows, or even more nonuniform flows in a compound bed, are very complicated because of the mass transfer and the amount of movement between the minor bed and the major bed (2005). These two phenomena, manifesting themselves in different ways, are sources of dissipation of additional energy from the flow. It can therefore be interesting to see the magnitude of these dissipations in the event that a hydraulic jump occurs in the compound bed. This is more interesting since the hydraulic jump is used precisely for the dissipation of energy. This additional dissipation is therefore more than welcome.

In other studies, presented by Benabdesselam et al. (2017), the authors provided dimensionless relations governing the sequence depth ratio and the relative energy loss of the hydraulic jump in a compound rectangular channel.

Roushangar et al. (2017) evaluated the capacity of the SVM approach for modeling hydraulic jump characteristics in three sharply enlarged dissipation basins. Various combinations of inputs based on the hydraulic characteristics and the geometry of the accessories were used to find the most suitable combination to model the hydraulic jump characteristics. Finally, the accuracy of the best SVM model was compared to existing conventional approaches.

The compactness of the hydraulic jump in the trapezoidal channel has been experimentally analyzed by Benmalek et al. (2022). The authors studied the effect of the compactness ratio on the conjugate depths and the surface profile.

This study aims to find empirical and experimental relationships of the jump sequence depth ratio as a function of the inflow Froude number and the jump compactness ratio in a compound rectangular channel. Thus, a form of the jump surface profile was proposed in two cases of flow. In the first case, the jump was formed in the minor canal. In the second case, the jump reached the major canal.

MATERIALS AND METHODS

The experimental channel shown in Figs. 1 and 2 comprises a supply basin connected to a measuring channel with a compound rectangular section by a circular PVC pipe with a diameter of 110 mm. The assembly functioned in a closed circuit, in which two parallel inserted pumps supply a convergent with open load in the measurement channel. The measuring channel of the compound rectangular section with a length of 6 m is connected with its downstream part to a second simple rectangular section channel, in which a rectangular weir is inserted without shovel height and with a lateral contraction allowing the direct measurement of the discharge flow. The compound rectangular channel is connected with its upstream part to a loaded box. The convergent role is to generate a high incident flow speed. The convergent exit section is variable, and its height corresponds to the initial jump's height h_1.

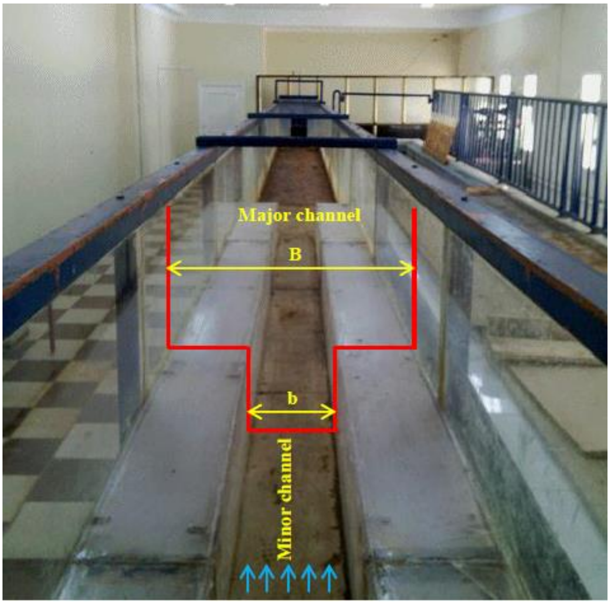

Figure 1: Compound rectangular section measurement channel

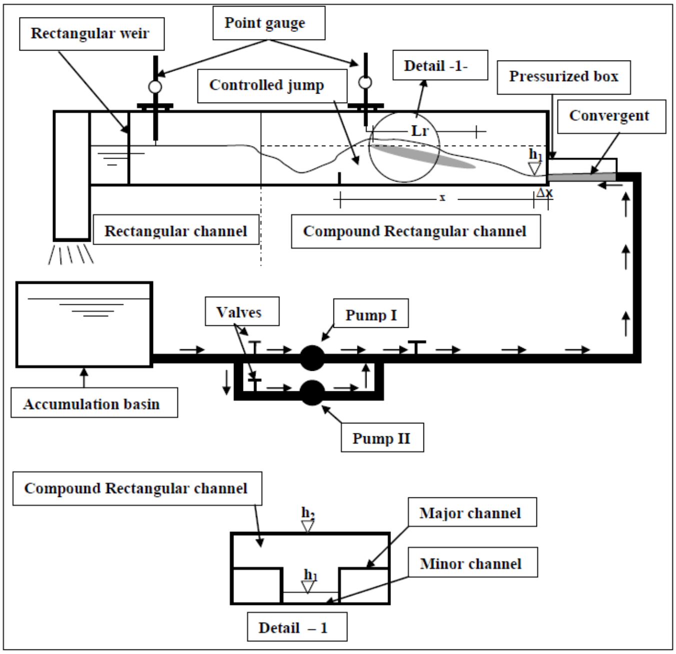

Figure 2: Simplified diagram of the measuring channel used for the experiment

The discharge flow Q and the depth h_2 are the only quantities that require specific equipment. However, the sill position x and its geometric height s are simply measured using graduated tape. The initial jump's height h_1 is assimilated to the opening of the convergence of Fig. 3 under various inflow heights (h_1=2 cm; 3 cm; 4 cm; 5 cm and 6 cm) after positioning the jump toe at approximately $\Delta x \approx 5$ cm. The water depth h_2 is measured by a double precision water level gauge, as shown in Fig. 4.

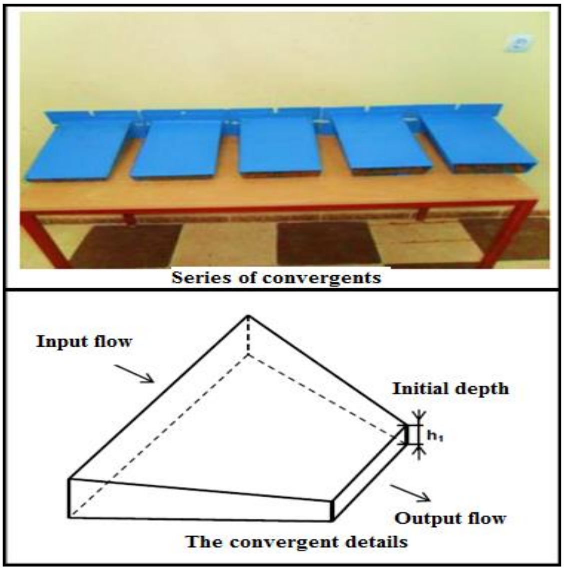

Figure 3: Convergent used in the experimental model

The h_2 values obtained were injected with the formula of Hachemi Rachedi (2006) for the flow meter with a rectangular weir. The water depths in the measurement channel were evaluated by a point gauge with the exception of the initial jump height, in which the value is assimilated to the convergent opening under load. The instrument is composed of a graduated metal ruler on one face and provided at its lower part with a vertical point (limnimetric point) whose role is to flush the water surface (Fig. 4). The reading on the point gauge is carried out in two stages: the first one was preceded by reading on the ruler graduation located immediately above the zero of the point gauge. The second one is carried out by reading the fiftieths number facing the division that coincides or closest to a ruler division.

Figure 4: Point gauge

The sills used in the experimental device (Fig. 5) possess a ferric rectangular form, where their fixations are ensured using a thin metal support (Fig. 6). To obtain a large number of measurement points, 18 thin sills with different heights were prepared: *s*=2 cm; 3 cm; 4 cm; 5 cm; 6 cm; 7 cm; 8 cm; 9 cm; 10 cm; 11 cm; 12 cm; 13 cm; 14 cm; 15 cm; 16 cm; 17 cm; 18 cm; 19 cm and 20 cm.

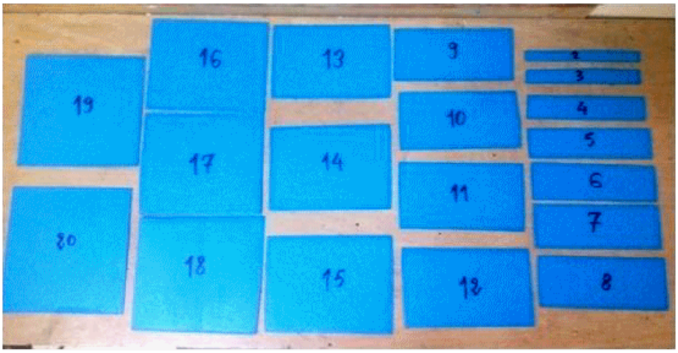

Figure 5: Thin sills tested

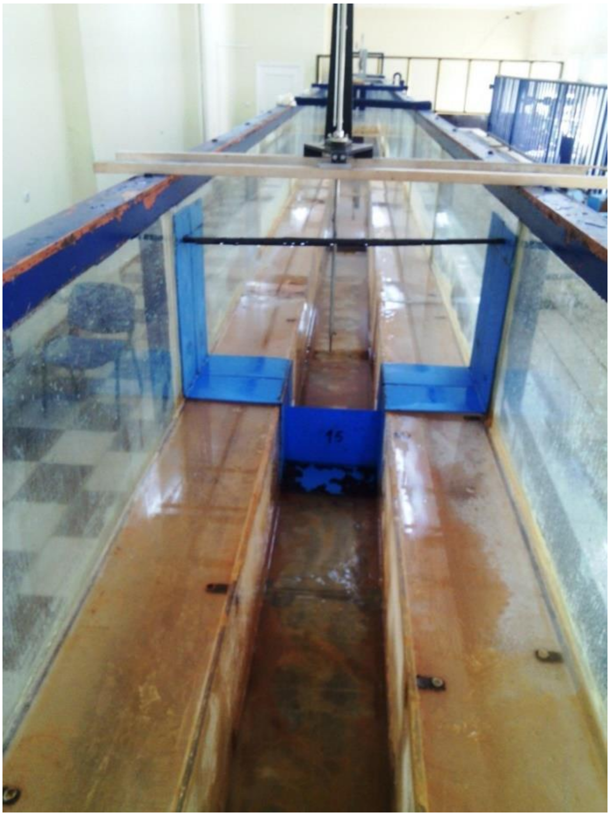

Figure 6: Sill support

DESCRIPTION OF THE EXPERIMENTAL MODEL

According to the bibliographic study, when the controlled jump is entirely formed in the dissipation basin for a geometric height of the sill and a length x of the basin (Fig. 3), the displacement of the sill downstream does not in any way modify the jump configuration, which allows the roller jump length Lr to be practically comparable to the sill position x.

On the other hand, the sill upstream displacement ($Lr/x>1$) causes jump compactness and leads to several configurations (Fig. 8). The main objective of this work is to determine the effect of a thin-walled sill on the hydraulic jump profile in a compound rectangular channel and to find an empirical equation expressing the variation in the jump sequence depth ratio $Y=h_2/h_1$ as a function of the Froude number Fr_1 and the compactness ratio δ defined as the classical roller length ratio Lr^* and the position x of the sill ($\delta=Lr^*/x$).

For this purpose, the cases have been distinguished where the flux occupies the majority of the compound rectangular channel (Fig. 7).

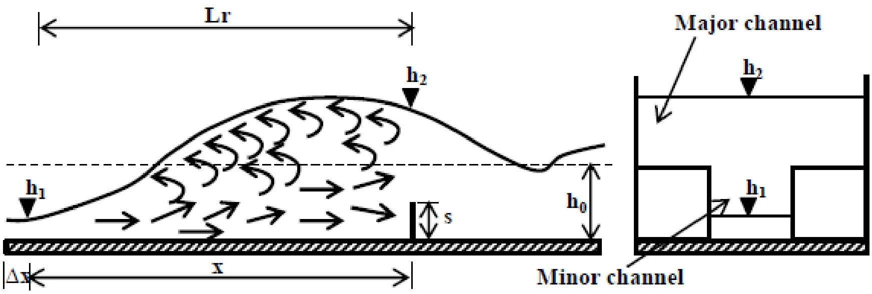

Figure 7: Geometric parameters of a compound rectangular channel

The different geometrical and hydraulic parameters obtained for this type of jump allowed the following dimensionless products to be composed: the inflow Froude number, the ratio $Y=h_2/h_1$ and the compactness ratio $\delta=Lr^*/x$, where Lr^* is the length of the classical jump roller. The Froude number Fr_1 in the case of a rectangular channel is given by Eq. (1):

$$Fr_1 = Q / \sqrt{b^2 h_1^3 g} \tag{1}$$

These dimensionless products can be linked by the functional relation f_1 (Fr_1, Y, δ) = 0. One of the objectives of this part of the study is to define the functional relationships f_1 through laboratory experiments. This makes it possible to evaluate the compactness jump ratio δ, knowing the pair of values (Fr_1, Y).

Fig. 8 shows different jump configurations that can also be obtained at increasing flow rates by fixing the sill heights, which generates a progressive distance reduction x between the jump toe and the sill position. This decrease is followed by a slight increase in the initial height h_1. The latter is only significant for relatively large distances Δx.

Four intervals of compactness ratio δ covering the whole range of experimental data were analysed. Each of them corresponds to an intermediate configuration of the controlled jump. $\delta \leq 0.90$; $0.91 \leq \delta \leq 1.11$; $1.12 \leq \delta \leq 1.32$; $1.33 \leq \delta \leq 1.53$; $1.54 \leq \delta \leq 1.74$. Each class of measures is represented by its center, as shown in Table 1.

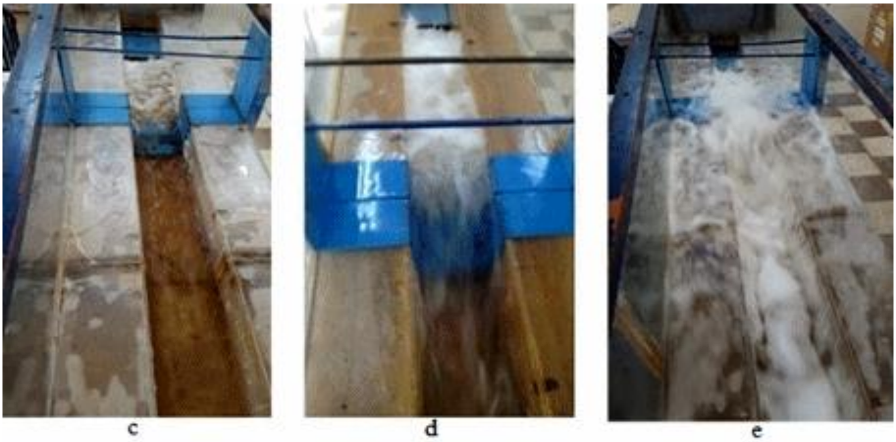

Figure 8: Different configurations of the controlled jump by sill, obtained at increasing discharge flow for a sill position x=72 cm, an initial height h_1=2cm and Δx≈5cm. c) Fr_1=5.00, s=6cm, h_2=13cm, δ=0.81. d) Fr_1=8.95, s=8cm, h_2=18cm, δ=1.09. e) Fr_1=10.55, s=10cm, h_2=20.5cm, δ=1.42

Table 1: Compactness class centers

Class	≤ 0.90	0.91–1.11	1.12–1.32	1.33–1.53	1.54–1.74
Center	-	1.01	1.22	1.43	1.64

The values of $\delta \leq 0.90$ correspond to the classical jump configuration. For a representative sample, we determine the flow discharge Q, the initial height h_1, the final height h_2, the sill height s, and the relative position toward the jump foot x. These make it possible to compose the following dimensionless products: the Froude number Fr_1 of the incident flow, the ratio $Y=h_2/h_1$ and the compactness ratio $\delta=Lr^*/x$, Lr^* being the classical jump roller lengths, which are given by the experimental relation of the relative classical roller length $Lr^*/h_1=f(Fr_1)$.

The classical roller values were experimentally determined using the relationship of the relative classical roller length ($\delta \leq 0.90$) as a function of the Froude number.

The adjustment of the function Lr^*/h_1 in Fig. 9 shows that the experimental data vary along a line given by Eq. (2).

$$Lr*/h_1 = 9.66Fr_1 - 31.87 \quad (2)$$

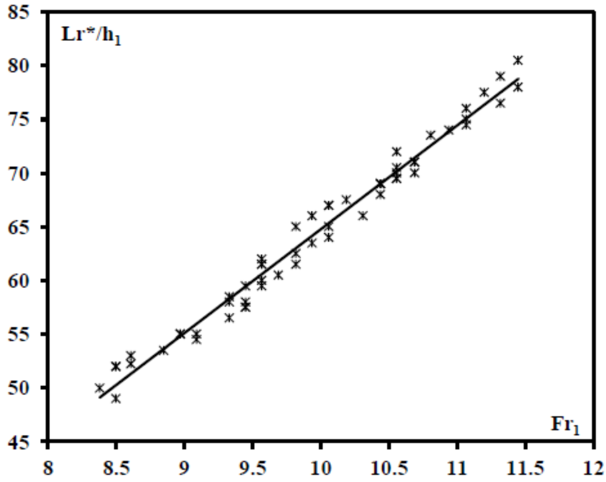

Figure 9: *Lr*/h₁=f(Fr₁)* experimental variation. (—) Model data

RESULTS AND DISCUSSION

Sequent depth ratio for δ > 0.90

Fig. 10 shows the experimental data and their adjustments. The curves always appear at a distance, as indicated by the shape of the adjustment curves. This distance was due to the contribution of the classical jump, where it started to be noticed ($\delta \geq 1.22$). Furthermore, for each compactness ratio δ relating to a given configuration of the projection, the experimental measurement points are adjusted around a linear type curve of the form $Y=aFr_1+b$.

For a given value of the inflow Froude number, the ratio Y decreases with increasing compactness ratio δ. Tables 2 group together the different coefficients of the adjustment lines of the experimental relation linking the ratio $Y=h_2/h_1$ of the heights combined with the Froude number Fr_1 of the incident flow for different compactness ratios.

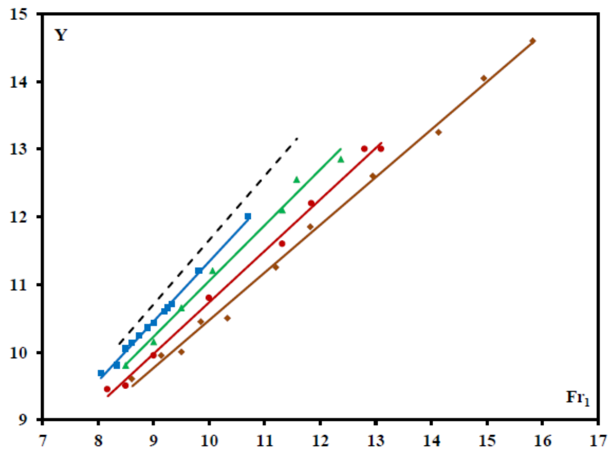

Figure 10: Variation in *Y* as a function of *Fr₁* for different average compactness ratios δ=(□) 1.01; (Δ) 1.22; (○) 1.43; (+) 1.64. (---) Classical jump (δ≤0.90)

Table 2: Coefficients of experimental relations resulting from the adjustment of the relation linking *Y* to the Froude number Fr_1 for different compactness ratios δ.

Ranges of δ	Linear equations	Correlation coefficients R^2
$0.90 \leq \delta \leq 1.11$	$Y = 0.89 Fr_1 + 2.49$	0.995
$1.12 \leq \delta \leq 1.32$	$Y = 0.82 Fr_1 + 2.82$	0.990
$1.33 \leq \delta \leq 1.53$	$Y = 0.76 Fr_1 + 3.14$	0.995
$1.54 \leq \delta \leq 1.74$	$Y = 0.70 Fr_1 + 3.42$	0.996

Table 2 shows that the slopes '*a'* of the straight lines gradually decrease from one configuration to another with an almost constant step. These observations show the possibility of the existence of a single linear type relation of the form $Y=aFr_1+b$, which group together four (04) intermediate controlled jump configurations linking the sequence depth ratio Y with the Froude number Fr_1 and the jump compactness ratio δ.

The coefficients "*a*" and "*b*" of the adjustment lines varied according to the compactness ratio, δ, as shown in Figs. 11 and 12.

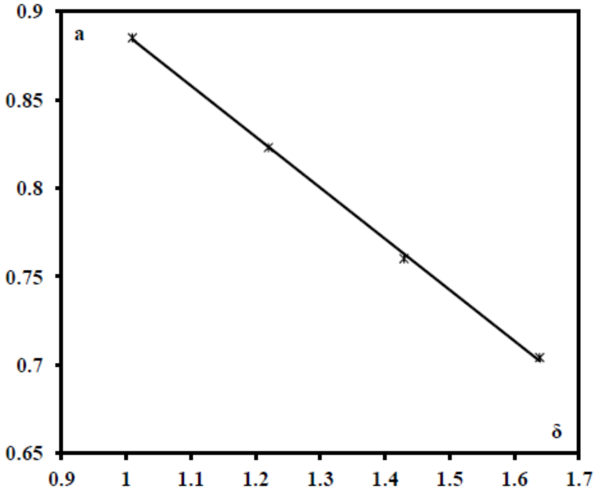

Figure 11: The coefficient "*a*" variation as a function of *δ*

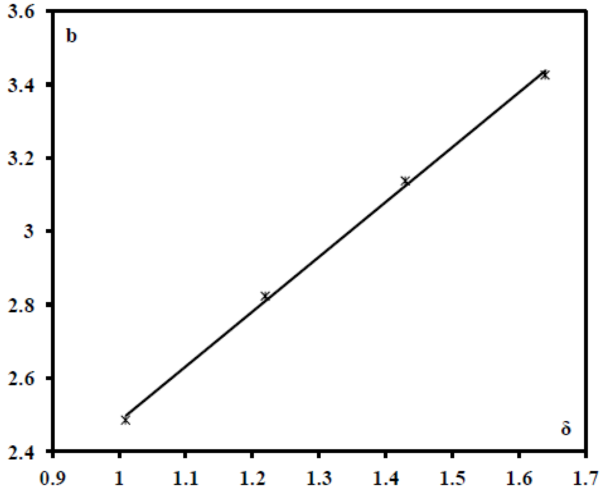

Figure 12: The coefficient "*b*" variation as a function of *δ*

Then, for all configurations of the controlled jump by the thin sill in a compound rectangular channel, a unique Eq. (3) of the form here, a term missing $\psi=f(Fr_1)$ is proposed, allowing the ratio $Y=h_2/h_1$ to be determined as a function of the inflow Froude number Fr_1:

Eq. (3) then proposes a unique relation of the form $\psi=f(Fr_1)$ that allows us to determine Y as a function of the inflow Froude number Fr_1 for all configurations of the controlled jump by a thin sill in a compound rectangular channel.

$$\psi = (1.18 - 0.29\delta)Fr_1 + (0.99 + 1.49\delta) \tag{3}$$

For a range of Froude numbers $8.05 \le Fr_1 \le 15.83$, the values of the compactness ratio are $0.91 \le \delta \le 1.74$. The graphical representation of the measurement points and the experimental equation ψ are shown in Fig. 13. The latter shows that the majority of experimental points accumulate around the fit line, which minimizes the relative error between the experimental data of Y and the function $\psi = (1.18\text{-}0.29\delta)\ Fr_1 + (0.99+1.49\delta)$.

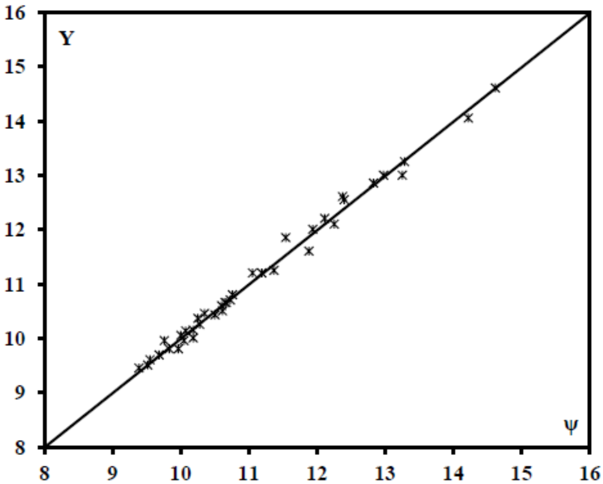

Figure 13: Experimental variation in the sequence depth ratio *Y* as a function of ψ.

The jump surface profile

For the range of h_1 varying from 2 to 5 cm, we have represented the surface profile $y=f(x)$, such that $y=[h(x)-h_1]/[h_2-h_1]$, $X=x/Lr^*$. Fig. 18 represents the jump surface profiles relative to each average value of the jump compactness, namely, $\delta \le 0.90$, $\delta=1.01$, $\delta=1.22$, $\delta=1.43$, and $\delta=1.64$.

Analysis of the experimental points corresponding to the classical jump (0.90) shows that the variation of the function $y=f(X)$ is the hyperbolic tangent of the equation $y=a\mathrm{Tanh}(bX)$ given by Eq. (4).

$$y = 1.19\mathrm{Tanh}[1.40X] \tag{4}$$

The graphic representations of the jump surface profiles are given in Fig. 14.

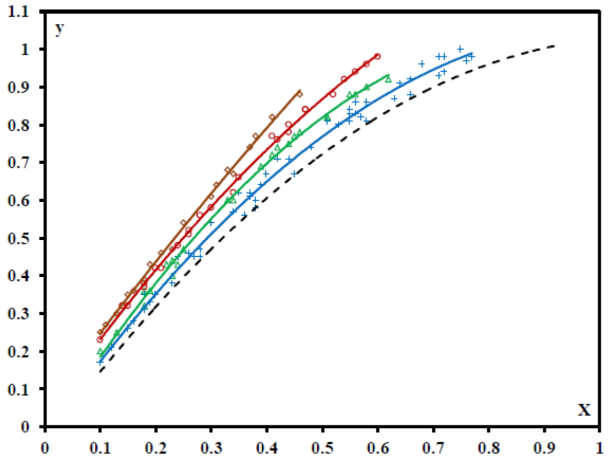

Figure 14: Experimental variation of the jump surface profile [$y=f(X)$] in the compound rectangular channel for four intermediate compactness ratios. (….) Classical jump according to the equation y=1.19Tanh[1.40X] ($\delta \leq 0.90$). (—) Adjustment curves for (□) δ=1.01; (Δ) δ=1.22; (×) δ=1.43 and (○) δ=1.64

As shown in Fig. 14, the greater the compactness ratio increases, the greater the coefficient value *"a"* increases, which influences the shape of the adjustment curves.

Table 3 groups together the different coefficients of the adjustment curves of the experimental relationships, linking $y=(h_x-h_1)/(h_2-h_1)$ of the jump surface to the relative ratio $X=x/Lr^*$, for different mean compactness ratios δ.

Table 3: Experimental values of X and y for four intermediate compactness ratios δ of the controlled jump

Ranges of δ	Linear equations	Correlation coefficients R^2
$0.91 \leq \delta \leq 1.11$	y =1.21Tanh[1.50X]	0.991
$1.12 \leq \delta \leq 1.32$	y =1.24Tanh[1.59X]	0.997
$1.33 \leq \delta \leq 1.53$	y =1.28Tanh[1.66X]	0.997
$1.54 \leq \delta \leq 1.74$	y =1.32Tanh[1.72X]	0.994

The coefficients *"a"* and *"b"* of Figs. 15 and 16 varied according to the compactness ratio δ.

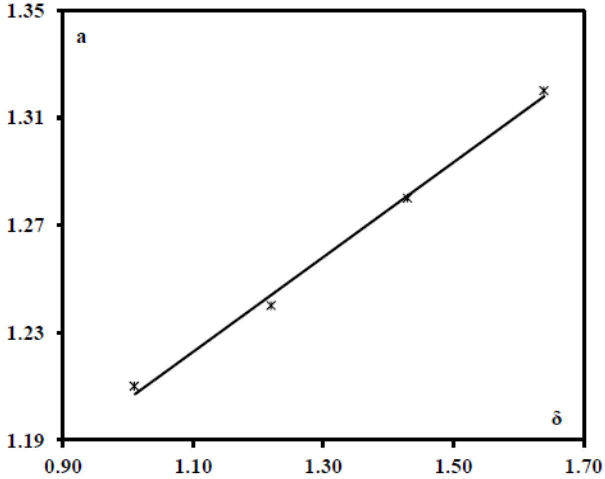

Figure 15: The coefficient "*a*" variation as a function of *δ*

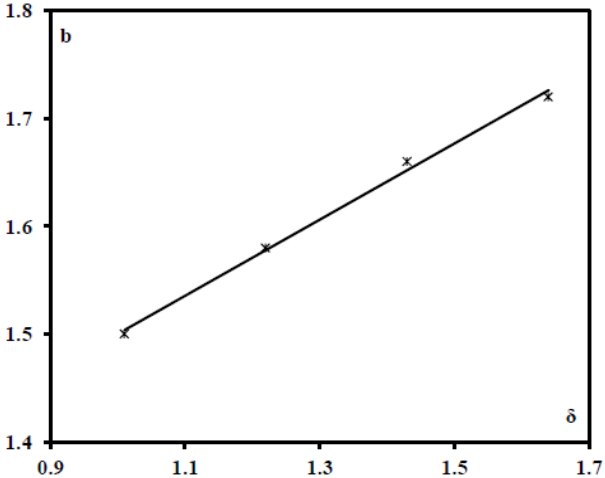

Figure 16: The coefficient "*b*" variation as a function of *δ*

The experimental relationship translating the variation of *y* as a function of *X* and the compactness ratio δ for $0.91 \leq \delta \leq 1.74$ is as follows:

$$\Phi = (0.18\delta + 1.03)Tanh[(0.35\delta + 1.15)] \tag{5}$$

If the compactness ratio δ is equal to 0.90 (classical jump), Eq. (5) gives Φ=1.19Tanh[1.46X], which implies that Eq. (4), corresponding to the classical jump.

The graphical representations of *y* as a function of Φ are given in Fig. 17.

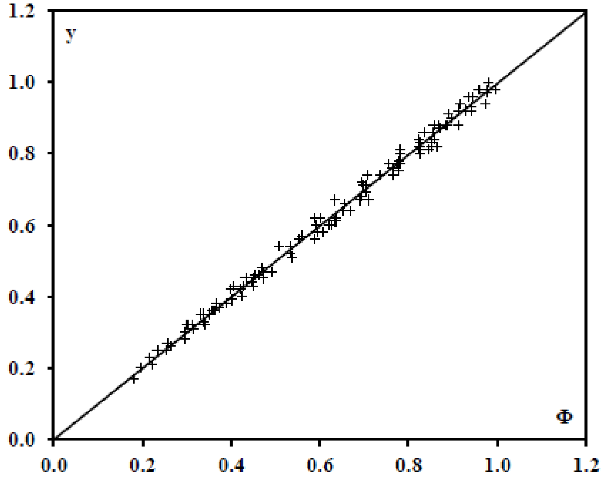

Figure 17: Experimental variation of the jump surface profile *y* as a function of *Φ*.

CONCLUSION

Through this study, an experimental analysis of the hydraulic jump compactness in a compound rectangular channel was proposed. The experimental analysis of the results for two parts of the channel, namely, the minor bed and the major bed, resulted in dimensionless empirical relationships expressing the variation of the sequence depth ratio Y as a function of the inflow Froude number Fr_1 and the compactness ratio δ defined as the classical roller length ratio Lr^* and the sill position x. Concerning the variation of Y, it was found that for a given value of the inflow Froude number Fr_1, the jump sequence depth ratio Y decreased with increasing compactness ratio δ. The experimental data of the jump surface profile $y=f(X)$ showed that this function is hyperbolic tangent, and for an important compactness ratio, the distance from the sill position decreases, which gave a minimal configuration of the stilling basins.

In general, the results obtained will be used to design better stilling basins.

Declaration of competing interest

The authors declare that they have no known competing financial interests or personal relationships that could have appeared to influence the work reported in this paper.

REFERENCES

ACHOUR B., AMARA L., MEHTA D. (2022a). Control of the hydraulic jump by a thin-crested sill in a rectangular channel - new experimental considerations, Larhyss Journal. No 50, pp. 31-48.

ACHOUR B., AMARA L. (2022b). Control of the hydraulic jump by a broad-crested sill in a rectangular channel, Part 1: new theoretical considerations, Larhyss Journal, to be published

ACHOUR B., AMARA L. (2022c). Control of the hydraulic jump by a broad-crested sill in a rectangular channel, Part 2: experimental validation, Larhyss Journal, to be published.

BAKHMETEFF B.A., MATZKE A.E. (1936). The hydraulic jump in terms of dynamic similarity, Transactions of the American Society of Civil Engineers, ASCE, Vol. 101, No 1, pp. 630-647.

BELANGER J.B. (1828). Essay on numerical Solution of some problems relative to steady flow in water, Carilian-Goehry, Paris.

BENABDESSELAM A., ACHOUR B., HOUICHI L. (2017). Hydraulic jumps in a straight rectangular compound channel; theoretical approach and experimental study, Larhyss Journal, No 29, pp. 323-340.

BENMALEK A., DEBABECHE M. (2022). Theoretical and experimental analysis of sequence depth ratio and energy loss in an abruptly enlarged trapezoidal channel, Larhyss Journal, No 49, pp. 67-84.

BENMALEK A., DEBABECHE M., ZAID Z. (2022). Experimental Study of the Hydraulic Jump Compactness in an Open Trapezoidal Channel, Advanced Materials Research, Transactions Tech Publications Ltd., Vol. 1168, pp. 123-137.

BIDONE G. (1828). Observations on the height of the hydraulic jump, a Report Presented in Meeting of Royal Academy of Science of Turin, pp. 21-80.

BOUSMAR D., RIVIERE N., PROUST S., PAQUIER A., MOREL R., ZECH Y. (2005). Upstream discharge distribution in compound-channel flumes, Journal of Hydraulic Engineering, ASCE, Vol.131, No 5, pp. 408-412.

HAGER W.H. (1993). Classical hydraulic jump: free surface profile, Canadian journal of civil engineering, Vol. 20, No 3, pp. 536-539.

KATEB S., DEBABECHE M., BENMALEK A. (2013). Experimental study of the effect of the positive step on a hydraulic jump in a trapezoidal channel, Canadian Journal of Civil Engineering. Vol. 40, No 10, pp. 1014-1018. Étude expérimentale de l’effet de la marche positive sur le ressaut hydraulique évoluant dans un canal trapézoïdal.

KHATTAOUI M. ACHOUR B. (2012). Hydraulic jump in a compound channel, Le Journal de l'Eau et de l'Environnement, No 20, In French.

LIU J.L., WANG Z.Z., LENG C.J., ZHAO Y.F. (2012). Explicit equations for critical depth in open channels with complex compound cross sections, Flow Measurement and Instrumentation, Vol. 24, pp. 13–18.

MOORE W.L. (1943). Energy loss at the base of a free overfall. Transactions of the American Society of Civil Engineers, ASCE, Vol. 108, No 1, pp. 1343-1360.

OMID M.H., ESMAEELI V. M., NARAYANAN R. (2007). Gradually expanding hydraulic jump in a trapezoidal channel, Journal of Hydraulic Research, Vol. 45, No 4, pp. 512-518.

ROUSHANGAR K., VALIZADEH R., GHASEMPOUR R. (2017). Estimation of hydraulic jump characteristics of channels with sudden diverging sidewalls via SVM, Water Science and Technology, Vol. 76, No 7, pp. 1614–1628.

WANG H., CHANSON H. (2015). Experimental study of turbulent fluctuations in hydraulic jumps, Journal of Hydraulic Engineering, Vol. 141, No 7, pp. 04015010-1-04015010-10.

WANOSCHEK R., HAGER W. H. (1989). Hydraulic jump in trapezoidal channel. Journal of Hydraulic Research, Vol. 27, No 3, pp. 429-446.

YASUDA Y., HAGER W. H. (1996). Hydraulic jump in channel contraction, Canadian journal of civil engineering, Vol. 22, No 5, pp. 925-933.

ZAHIRI A., DEHGHANI A. A. (2009). Flow Discharge Determination in Straight Compound Channels Using ANNs, World Academy of Science, Engineering and Technology, International Journal of Computer, Electrical, Automation, Control and Information Engineering, Vol. 58, pp. 12-15.